



Effects of process parameters on microstructure and wear resistance of TiN coatings deposited on TC11 titanium alloy by electrospark deposition

Xiang HONG, Ke FENG, Ye-fa TAN, Xiao-long WANG, Hua TAN

College of Field Engineering, PLA University of Science and Technology, Nanjing 210007, China

Received 10 May 2016; accepted 23 November 2016

Abstract: In the present study, the effects of process parameters (output voltage x , nitrogen flux l and specific strengthening time s) on the microstructure and wear resistance properties of TiN coatings prepared by electrospark deposition (ESD) were investigated systematically. The microstructure of the coatings was characterized for thickness (TOC), content of TiN (CON) and porosity (POC). A statistical model was developed to identify the significant factors affecting the microstructure and wear resistance of the coatings. The results show that the output voltage x and nitrogen flux l present significant effects on majority of the evaluation indexes such as TOC, friction coefficient (COF) and wear mass loss (I_d), while the specific strengthening time s has a significant effect on POC and a small effect on the other indexes. The optimal process parameters were obtained as follows: output voltage (x , 60 V), nitrogen flux (l , 15 L/min) and specific strengthening time (s , 3 min/cm²). The variation of wear mass loss (I_d) by the variation of the output voltage (x) and nitrogen flux (l) is attributed to the change of wear mechanisms of TiN coatings. The main wear mechanism of TiN coating prepared under optimal process parameters is micro-cutting wear accompanied by micro-fracture wear.

Key words: electrospark deposition (ESD); TiN; coating; wear resistance; statistical model; process parameters

1 Introduction

Titanium alloys have many advantages such as low density, high specific strength, excellent corrosion resistance and biocompatibility [1–3]. Thus, they have been widely applied to aerospace, chemical engineering, metallurgy, medicine and nuclear industries. However, titanium alloys limit their further application due to their poor tribological properties such as high friction coefficient and prone to adhesive wear, leading to their failure in the early service stage [4]. Surface modification and treatment of titanium alloys by using methods such as physical or chemical vapor deposition (PVD, CVD) [5,6], ion implantation [7], thermal oxidation [8], and magnetron sputtering techniques [9] have achieved good results. However, the applications of these surface technologies are restricted for the generation of some adverse effects on the titanium alloys. For example, due to the high temperature, it is easy to cause the deformation of the substrates by the nitriding, sulfurizing and CVD process. The equipment of PVD is relatively complicated, and it is hard to carry on the processing for the large scale parts because of the

necessary vacuum or gas environment for PVD. The coating deposited by magnetron sputtering method is relatively thin with low efficiency [10]. Therefore, it is urgent to prepare excellent coatings on titanium alloys bonding with substrate metallurgically while minimizing the total heat input into the substrate.

Electrospark deposition (ESD) is a typical surface modification technology with high energy density and low heat input, which has been widely used in the preparation of modified strengthening coatings [11–13]. Utilizing the high energy pulsed discharge between electrode and metallic substrate, the ESD process can deposit the melting electrode materials onto the substrate to accomplish metallurgical reaction with substrate. Currently, several coatings have been deposited on titanium alloys by ESD process. WANG et al [14] deposited WC92–Co8 hard alloy coating on titanium alloys by ESD and studied the microstructure and interface of the coatings. The microhardness of coating reached HV 1192, but the coating was thin (26.3–56.12 μm) and inhomogeneous. TANG et al [15] carried out ESD in the conditions of air, nitrogen gas atmosphere and silicone oil respectively using a graphite electrode on titanium alloy. The results showed that the ESD coating

treated in silicone oil exhibited better biocompatibility and biological activity in comparison with other conditions, but the silicone oil dielectric environment restricted to the application for large mechanical parts by the ESD. HAO et al [16] prepared TiN coating on TC4 titanium alloy by ESD, but the coating was relatively thin (12.1–24.3 μm) and the influence of process parameters on the properties of the coatings had not been studied.

Based on a large number of experiments on developing coatings on titanium alloys by ESD, it is evident that the process parameters have great effects on the properties of coatings. In view of the excellent properties of TiN coating such as high hardness, high strength, low friction coefficient, anti-wear and corrosion resistance, it is a promising surface coating to strengthen the titanium alloy. Thus in this work, the TiN coatings were deposited under different process parameters and the effects of parameters on microstructure, mechanical properties and tribological properties of the coatings were studied systematically to provide the theoretical basis and technical support for the further engineering applications of titanium alloys.

2 Experimental

2.1 Materials and processing

Titanium alloy plate of TC11 with the dimension of 10 mm \times 10 mm \times 3 mm was selected as the substrate material. The chemical composition of TC11 is listed in Table 1. The pure titanium rod of TA2 with diameter of 3 mm was used as the electrode. Prior to ESD, the substrate specimens and the electrode tip were ground with 800-grit SiC paper to remove the oxide films and then rinsed with acetone to remove surface oil. The experiments were carried out by a 3H-ES ESD deposition machine. The schematic diagram of ESD process is shown in Fig. 1. The deposition gun connects with high frequency power supply through the wire. The electrode rod is fixed by the clamp in the deposition gun and rotates with high-speed of 2500 r/min driven by the deposition gun. The deposition gun is hold by hands with a certain angle (30° to 45°) to the substrate surface, moving back and forth in the speed of 0.001 m/s.

Table 1 Chemical composition of TC11 titanium alloys (mass fraction, %)

Al	Mo	Zr	Si	Fe	O	Ti
6.32	3.29	1.79	0.23	0.077	0.096	Bal.

2.2 Factorial experimental design

A factorial experimental method was applied to investigating the factors on the properties of wear resistance of the coatings. In this study, the influence of

three factors (output voltage, nitrogen flux and specific strengthening time labeled as x , l and s respectively) on the microstructure and wear resistance of TiN coatings was been studied systematically. The Taguchi orthogonal array (TOA) was used to design the experiment. Three levels at same intervals of the parameters were selected as experiment factors, and its distribution is shown in Table 2. A standard L_93^4 orthogonal table containing nine test combinations was used to analyze the importance of four independent factors with three levels, the lists indicate the factor levels, and the line has determined the concrete test plan.

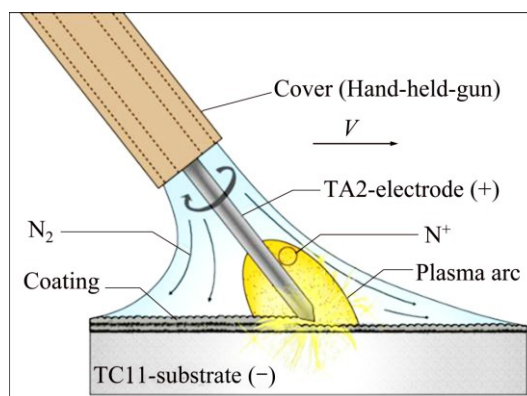


Fig. 1 Schematic diagram of preparing in-situ TiN coatings on TC11 by ESD [17]

Table 2 Factors and their levels for TiN coatings deposition in experimental design

Level	Output voltage, x/V	Nitrogen flux, $l/(L \cdot \text{min}^{-1})$	Specific strengthening time, $s/(\text{min} \cdot \text{cm}^{-2})$
1	40	5	3
2	60	10	4
3	80	15	5

2.3 Surface analysis

The microstructure and the worn surface of ESD coatings were observed by the scanning electron microscope (SEM) of QUANTA 200. In addition, the phase composition was identified by a D/max 2500/PC type X-ray diffractometer with Cu target operated at 40 kV and 200 mA. The microhardness of the coatings was measured using the DHV-1000 microhardness tester under the load of 1.96 N with a dwell time of 15 s. The surface roughness of the coatings was measured by Sufcorder SE300 surface roughometer. Using MATLAB software programming to calculate the porosity of the coating based on the image gray method.

2.4 Tribological tests

Tribological tests of ESD coatings sliding against a GCr15 ball with diameter of 4 mm and surface roughness of 0.05 μm were carried out by an HT-500 ball-on-disk

tribometer in dry friction. The tribological tests were conducted in normal atmospheric temperature (25 °C) with a constant speed of 0.42 m/s under a normal load of 4 N. The sliding friction time was 30 min. The mass losses of the specimens were measured by an ATB120–4M electric analytical balance with the accuracy of 0.1 mg.

2.5 Statistical methods

A three-way analysis of variance (ANOVA) was applied to studying the influence of output voltage, nitrogen flux and specific strengthening time on the microstructure and wear resistance of the coatings. The *F* ratio was calculated by the following equations.

$$CF = \frac{(\sum y)^2}{n} \tag{1}$$

$$SS_x = \frac{(\sum X)^2}{n_x} - CF \tag{2}$$

$$SS_l = \frac{(\sum L)^2}{n_l} - CF \tag{3}$$

$$SS_s = \frac{(\sum S)^2}{n_s} - CF \tag{4}$$

$$SS_T = (\sum y^2) - CF \tag{5}$$

$$\text{Error} = SS_T - SS_x - SS_l - SS_s \tag{6}$$

$$MS = SS/df \tag{7}$$

$$F = MS/MS_{\text{Error}} \tag{8}$$

where *CF*, *SS*, *MS* and *df* denote the correction factor, sum of squares, mean of squares and degrees of freedom

respectively. $\sum X$, $\sum L$ and $\sum S$ are the sum of totals representing the output voltage, nitrogen flux and specific strengthening time, respectively. Indices representing the levels in the output voltage, nitrogen flux and specific strengthening time are *x*, *l* and *s*, respectively. *n* and *y* denote the total number of experiments and the indicator in each experiment respectively. The subscript *T* denotes the treatment of each factor.

3 Results and discussion

3.1 Characterizations of coatings

The L_93^4 orthogonal table for the experiments and the results are shown in Table 3; where column *e* is error column, TOC is the thickness of the coating, CON is the contents of TiN in the coating, POC is the porosity of the coating, COF is the friction coefficient of the coating, *I_d* is the wear mass loss of the coating, and *R_j* is the range.

The range analysis can determine the significance of each factor on the indicators. Calculated *R_j* are listed in Table 3, and also plotted in Fig. 2. As can be seen, the output voltage *x* has significant effects on majority of the evaluation indexes, including the TOC, CON, COF and *I_d*. Besides, the nitrogen flux *l* also presents obvious effects on majority of the indexes such as CON, TOC, COF and *I_d*, while the specific strengthening time *s* has significant effect on POC and has minor effect on the other indexes.

As to the main index wear mass loss *I_d* corresponding to the wear resistance properties of the coatings, it is significantly affected by the output voltage *x* and nitrogen flux *l*, and the value of wear mass loss *I_d*

Table 3 L_93^4 orthogonal table for experiments and results

No.	Factor				Result				
	<i>x</i>	<i>l</i>	<i>e</i>	<i>s</i>	TOC/(Ra, μm)	CON/μm	POC/%	COF	<i>I_d</i> /mg
1	1	1	1	1	32	52	2.0	0.32	0.55
2	1	2	2	2	33	61	3.4	0.29	0.52
3	1	3	3	3	35	73	4.6	0.23	0.46
4	2	1	2	3	51	54	4.1	0.28	0.46
5	2	2	3	1	53	65	2.4	0.22	0.41
6	2	3	1	2	56	75	3.7	0.21	0.40
7	3	1	3	2	41	57	3.2	0.30	0.48
8	3	2	1	3	42	68	4.1	0.27	0.47
9	3	3	2	1	44	77	2.6	0.25	0.42
<i>R_j</i> -TOC	20	3.67	0.66	0.66					
<i>R_j</i> -CON	5.33	20.67	1	0.67					
<i>R_j</i> -POC	0.1	0.53	0.13	1.95					
<i>R_j</i> -COF	0.043	0.107	0.023	0.007					
<i>R_j</i> - <i>I_d</i>	0.21	0.19	0.05	0.01					

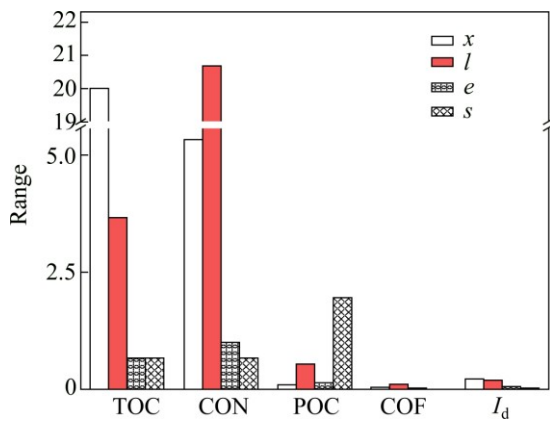


Fig. 2 Comparisons on R_j values of TOC, CON, POC, COF and I_d , respectively within selected ranges of x , l and s

reaches minimum at the level two of output voltage x and level three of nitrogen flux l , respectively. For the minor effect specific strengthening time s , the wear mass loss I_d reaches minimum at level one. Thus, by the above range analysis, the optimal process parameters for the preparation of TiN coating by ESD can be obtained as follows: output voltage (x , 60 V), nitrogen flux (l , 15 L/min) and specific strengthening time (s , 3 min/cm²), respectively.

The main effect plot for TOC of the coatings is shown in Fig. 3. The fluctuation of the coating thickness by output voltage x is bigger than that of other three factors, indicating that the thickness of the coating is greatly affected by the output voltage. With the increasing of output voltage, the thickness of the coating increases firstly and then decreases. The coating thickness reaches the maximum when the output voltage is on level two (60 V).

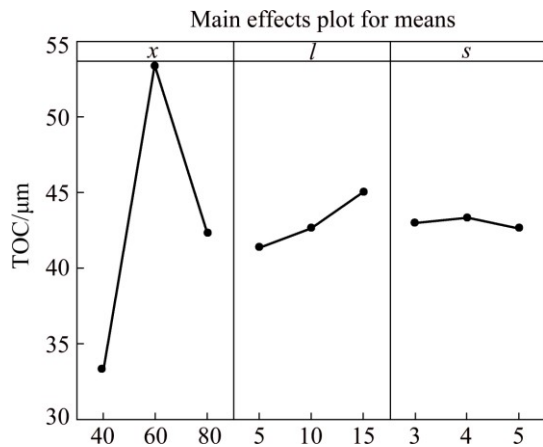


Fig. 3 Main effects plot for TOC of coatings (Units of x , l and s are in V, L/min and min/cm², respectively)

Figure 4 shows the cross section morphologies of the coatings under different output voltages. It can be seen that when the output voltage is moderate (60 V), the

coating thickness is the largest (55 μm) with a few micro-cracks. Besides, the coating is dense and uniform, bonding with substrate metallurgically [17]. However, if the output voltage is too low (40 V), the coating thickness is in the range of 30–35 μm, which is thinner than that of moderate condition (60 V). In excessive voltage condition (80 V), the coating thickness is 45–50 μm, which is also smaller than that of output voltage of 60 V. Meanwhile, the interface between the coating and the substrate appears many transverse micro-cracks, indicating that the bonding strength between the coating and substrate becomes worse.

The total heat energy increases when the output voltage is increased from 40 to 60 V due to the

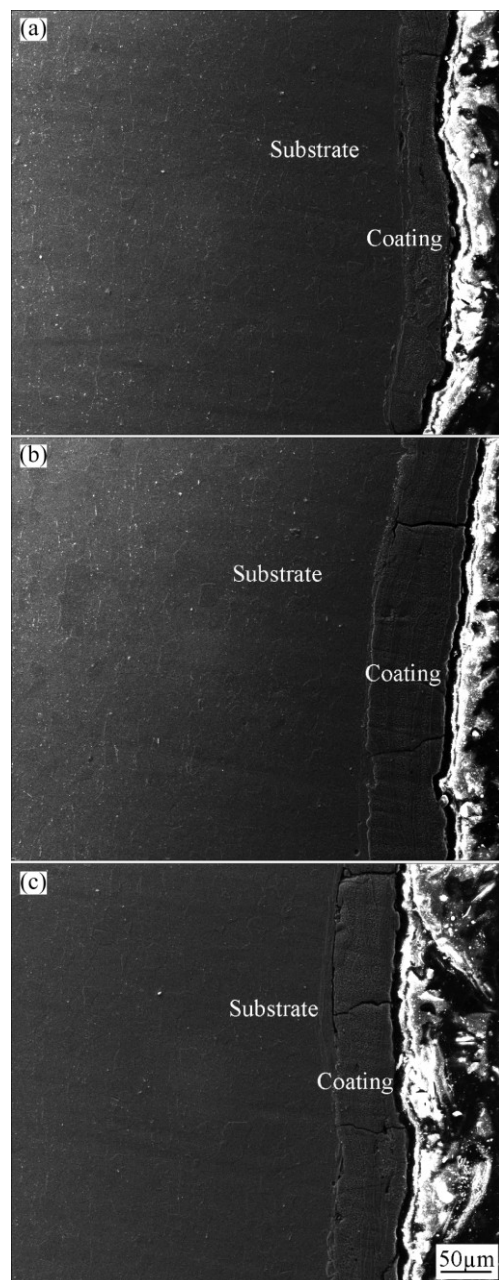


Fig. 4 Cross section morphologies of coatings under different output voltages: (a) 40 V; (b) 60 V; (c) 80 V

increasing of instantaneous pulse energy. The mixing and solidification between molten droplets and molten pools are severer than before, so the thickness of the coating is increased. However, in excessive output voltage condition (80 V), the instantaneous pulse energy and the energy of the plasma channel increase rapidly, leading to a great speed impacting on the surface of the substrate and the sharp splashing of liquid in the molten pool, which is not beneficial to the deposition of thick coating. And the thermal stress of the coating accumulates too fast due to the high output voltage, which may result in vertical and horizontal micro-cracks. In the reciprocating contact of electrode and substrate, the micro-crack propagation may cause the coating peeling off, which is not beneficial to the forming of coating.

The main effect plot for CON of the coatings is shown in Fig. 5. The data points in the l column follow a positive trend indicating that the CON increases from 5 to 15 L/min. Hence, the 15 L/min is the best amongst the levels. Besides, the fluctuation of the CON with the increase of l is the largest in comparison with other levels, indicating that the CON is greatly affected by the nitrogen flux.

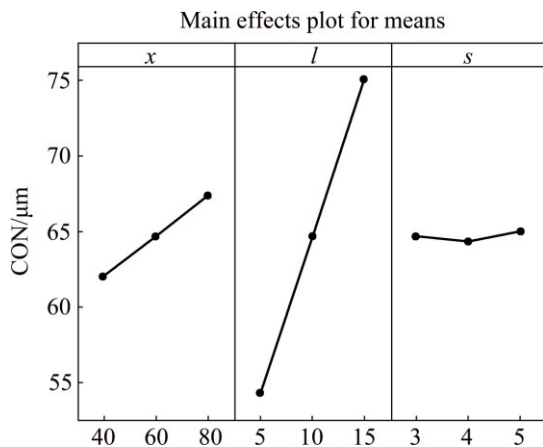


Fig. 5 Main effects plot for CON of the coatings (Units of x , l and s are in V, L/min and min/cm^2 , respectively)

The X-ray diffraction patterns of the coatings prepared in different nitrogen fluxes are illustrated in Fig. 6. The coating is mainly composed of Ti_2N , $\alpha\text{-Ti}$, TiO and TiN phases, which may be changed with the nitrogen flux. When nitrogen flux is small (5 L/min), insufficient nitrogen flux exposes the molten titanium alloy to the atmosphere of high temperature and leads to the reaction between Ti and O in air, which ultimately leads to the developing of TiO phase. The mass fraction of TiN phase in the coating can be measured by using MDI Jade software and theoretical techniques which are called K -value method or RIR -value method [18]. The results show that the mass fraction of TiN phase in the coating is about 52%. As can be seen, the $\text{Al}_3\text{Ti}_{0.8}\text{V}_{0.2}$ and

$\text{TiC}_{0.5}\text{N}_{0.1}$ compounds are generated when the nitrogen flux is 10 L/min, and the mass fraction of TiN is about 61%. When the nitrogen flux is 15 L/min, the coating is mainly composed of TiN , Ti_2N and TiO , in which the mass fraction of TiN is as high as 71%. The microhardnesses of the coating at 5 L/min and 10 L/min are $\text{HV}_{1.96}$ 872 and $\text{HV}_{1.96}$ 1234, respectively. And the microhardness of the coating at 15 L/min is also the maximum ($\text{HV}_{1.96}$ 1731), indicating that the increasing of TiN content in the coating is beneficial to improving the microhardness of the coating.

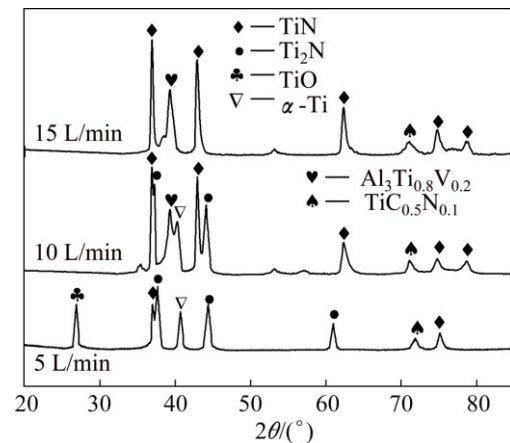


Fig. 6 X-ray diffraction patterns of coatings prepared in different nitrogen fluxes

The main effect plot for POC of the coatings is shown in Fig. 7. Obviously, the data points in the s column follow a positive trend, indicating that the POC increases from 3 to 5 min/cm^2 . Hence, the 3 min/cm^2 is the best amongst the levels. With the increase of the specific strengthening time, the porosity of the coating increases and the fluctuation range is larger than that of the other three factors, indicating that of the specific strengthening time has a great effect on the porosity of the coating. Besides, the fluctuation of the POC with the

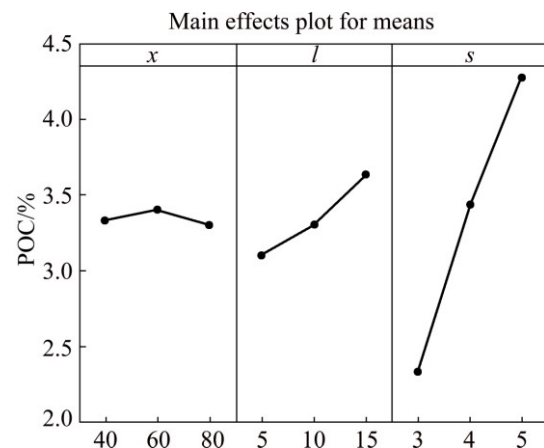


Fig. 7 Main effects plot for POC of coatings (Units of x , l and s are in V, L/min and min/cm^2 , respectively)

increases of s is the largest in comparison with other levels, indicating that the POC is greatly affected by specific strengthening time.

Figure 8 shows the cross section morphologies of the coating at different specific strengthening time s . When the specific strengthening time s is small (3 min/cm^2), the coating is dense and uniform, the porosity is about 2.1% (Fig. 8(a)). With the increasing of the specific strengthening time s , the micro-holes and micro-cracks increase (Fig. 8(b)), the porosity is about 3.6%. Especially when excessive specific strengthening time s is 5 min/cm^2 , a lot of transverse micro-cracks emerge between the coating and the substrate, and the coating is fractured as shown in Fig. 8(c), the porosity is about 4.8%. In the ESD process, the high speed rotating electrode and the substrate continually collide with each other to produce a spark. The molten electrode droplets on the surface of substrate are rapidly cooled and

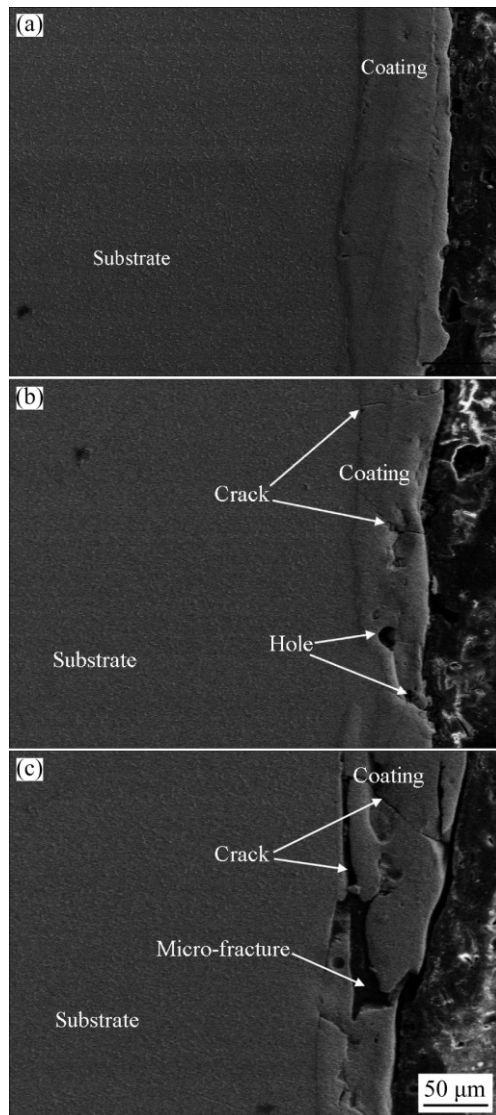


Fig. 8 Cross section morphologies of coating at different specific strengthening time s : (a) 3 min/cm^2 ; (b) 4 min/cm^2 ; (c) 5 min/cm^2

solidified. However, the accumulated residual tensile stress may exceed the yield strength of the coating [19], which results in the development and propagating of micro-cracks, and then leads to the peeling phenomenon and holes in the coating. Moreover, because TiN is hard with low toughness, the coatings are more prone to generate micro-cracks under the continuous action of thermal stress and the mechanical impact of electrode.

3.2 Wear resistance of coatings

Table 4 shows the results of the variance analysis. The significances of the effects on the major indexes can be determined. As can be seen, the SS means the sum of the deviation squares, MS means the mean of the squares, df is the freedom of the effects, F is the ratio of the variance; $F_{0.05}(2,2)$ and $F_{0.01}(2,2)$ are the judgment criteria for the significances of the effects on the factors. If F is larger than $F_{0.01}(2,2)$, the effect is very significant; if the F ratio is between $F_{0.01}(2,2)$ and $F_{0.05}(2,2)$, the effect is significant; if the F ratio is smaller than $F_{0.05}(2,2)$, the effect is insignificant. Based on the above descriptions, it is found that the priority levels are similar to the results of the range analysis: the effect of output voltage x on the TOC and I_d indexes are very significant, the effect of nitrogen flux l on the CON, COF and I_d indexes are also very significant. Also, the effect of specific strengthening time s on the POC index is very significant while is insignificant on the COF indexes.

According to the range analysis and ANOVA analysis of the effects of output voltage x , nitrogen flux l and specific strengthening time s on the TOC, CON, POC, COF and I_d indexes of the coatings, it is clear that the factors have significant effects on the microstructure and wear resistance properties of TiN coatings. As to the main indexes COF and I_d , it is significantly affected by output voltage x and nitrogen flux l , thus a further detail study was performed on the effects of two factors on the wear resistance of the coatings.

The variations of COF and I_d of the coatings by output voltage x and nitrogen flux l are shown in Fig. 9. As can be seen, A1, A2, A3 and A4 are the four levels of two factors, which are 40, 60, 80, 100 V and 5, 10, 15, 20 L/min, respectively. When the output voltage x and the nitrogen flux l increase, the COF decreases firstly and then increases, and it reaches the minimum at the level of A2 and A3, respectively. When the output voltage x is increased from level A1 to A2, the wear mass loss reaches minimum, which is only 0.42 mg. The coating deposited by ESD process is metallurgically bonded with substrate, but the interface is still the weak area of the coating system. The thick coating may effectively reduce the interface stress and the generation possibility of micro-cracks under the combination actions of normal

Table 4 Analysis of variance (ANOVA) for coating

Index	Factor	<i>df</i>	<i>SS</i>	<i>MS</i>	<i>F</i>	<i>F</i> _{0.05(2,2)}	<i>F</i> _{0.01(2,2)}	Significance
TOC	<i>x</i>	2	602	301	451.61	19	99	**
	<i>l</i>	2	20	10	15.01	19	99	
	<i>e</i>	2	1.333	0.667				
	<i>s</i>	2	0.667	0.333	0.51	19	99	
CON	<i>x</i>	2	42.667	21.333	21.34	19	99	*
	<i>l</i>	2	640.667	320.333	320.49	19	99	**
	<i>e</i>	2	1.999	1				
	<i>s</i>	2	0.667	0.333	0.33	19	99	
POC	<i>x</i>	2	0.015	0.008	0.61	19	99	
	<i>l</i>	2	1.099	0.549	43.96	19	99	*
	<i>e</i>	2	0.025	0.013				
	<i>s</i>	2	5.642	2.821	225.68	19	99	**
COF	<i>x</i>	2	0.0032	0.0016	52.46	19	99	*
	<i>l</i>	2	0.0074	0.0037	121.31	19	99	**
	<i>e</i>	2	0.00006	0.00003				
	<i>s</i>	2	0.0007	0.00035	11.48	19	99	
<i>I</i> _d	<i>x</i>	2	0.01032	0.00516	114.67	19	99	**
	<i>l</i>	2	0.00938		104.22	19	99	**
	<i>e</i>	2	0.00009					
	<i>s</i>	2	0.00211		23.44	19	99	*

* means the *F* ratio value is even larger than *F*_{0.05} (2, 2) and smaller than *F*_{0.01} (2, 2) and the influence of such factor is significant; ** means the *F* ratio value is even larger than *F*_{0.01} (2, 2) and the influence of such factor is very significant

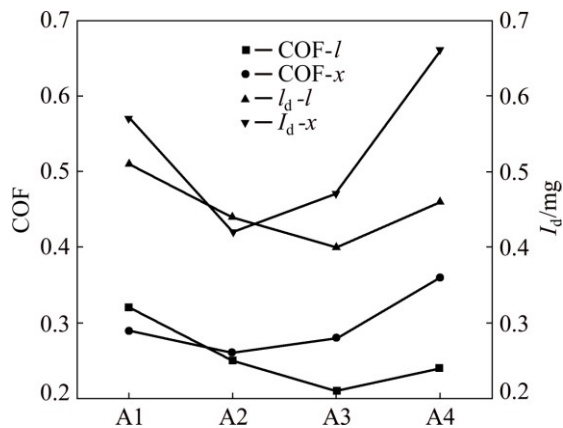


Fig. 9 Variation of COF and *I*_d with output voltage *x* and nitrogen flux *l* on four levels

load and friction force. Thus, it can avoid the occurrence of delamination failure of the coating in friction process. The wear mass loss decreases when the nitrogen flux *l* increases from level A1 to A3. According to the orthogonal analysis mentioned above, the CON is significantly affected by nitrogen flux *l*, so with the increasing of nitrogen flux *l*, the CON increases. Therefore, the microhardness of the coating increases and the mass loss decreases. But when with excessive nitrogen flux *l* (20 L/min), it may increase the velocity of

nitrogen flux released from deposition gun, so it is prone to producing turbulence on the surface of the coating, which leads to the generation of the micro-cracks and micro-holes in the coating, thus the mass loss of the coating increases.

Figure 10 shows the worn surfaces of the coatings under different output voltages. When the output voltage is 40 V, it is clear that deep furrows and serious plastic deformation distributed on the worn surface (Fig. 10(a)). So the main wear mechanism is multi-plastic deformation wear and micro-cutting wear, which is similar to the wear mechanism of TC11, indicating that the coating may be worn out and exposed to the surface of the substrate in the wear process, and the subsequent friction process is actually between titanium alloy substrate and the friction counterpart of GCr15 ball.

When the output voltage is increased (60 V), the worn surface is relatively smooth (Fig. 10(b)), in which the furrows become shallow, indicating that the resistance to micro-cutting wear ability of the coating is enhanced. In the friction process, because the coating withstands the dual action of normal load and shear force by the counterpart of GCr15 steel ball, the hard and brittle coating materials may peel off and become debris

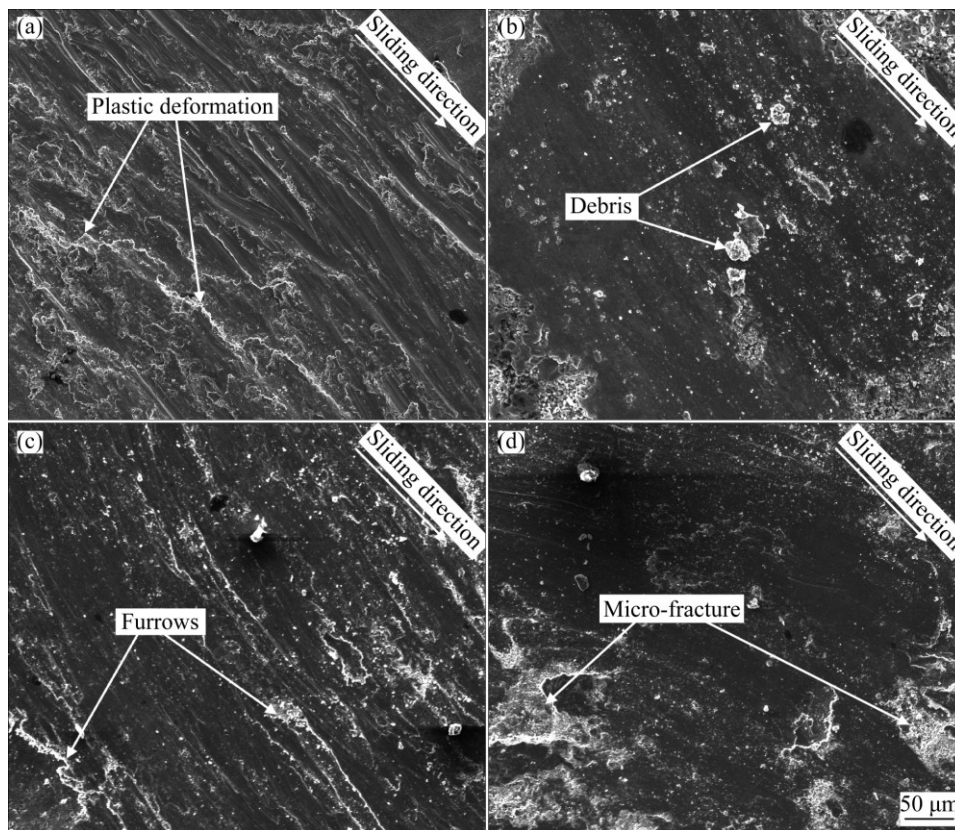


Fig. 10 Wear morphologies of coatings under different output voltages: (a) 40 V; (b) 60 V; (c) 80 V; (d) 100 V

in reciprocating extrusion and sliding process between the contact zone, resulting in furrows and micro-cutting traces [20]. As seen from Fig. 10(c), with the increasing of output voltage, the TiN content and microhardness of the coating are increased, which inhibits the ploughing effect caused by the counterpart of GCr15 and the abrasive wear by debris, so the worn surface of the coating becomes smooth. Also, the furrows on the worn surface of the coating under the condition of 80 V (Fig. 10(c)) are more obvious than that under the condition of 60 V (Fig. 10(b)).

When the output voltage is too large (100 V), the worn surface of coating appears some peeling pits (Fig. 10(d)), indicating that the micro-fracture wear occurred in the coating. When the output voltage is too large, the bonding strength between the coating and substrate becomes worse due to the transverse micro-cracks and other defects appear on the worn surface. The micro-cracks are easily to propagate under the dual effects of the vertical normal stress and the lateral shear force, resulting in the fracture of the coating, thus the wear mass loss increases.

Figure 11 shows the worn morphologies of the coatings prepared under different nitrogen fluxes. When nitrogen flux is 5 L/min, it is clear that the plastic deformation and ploughing traces appear on the surface of the coating (Fig. 11(a)). The amount of nitrogen ions

produced by high frequency pulsed discharge in low nitrogen flux condition is small; therefore, the amount of the nitrogen ions diffused into the molten pool is small. Thus, the contents of Ti_2N and TiN phases are small, which may decrease the microhardness of the coating, so the multi-plastic deformation wear and micro-cutting wear of the coating become serious. With the increasing of nitrogen flux (10 L/min), it can be seen from Fig. 11(b) that the furrows and plastic deformation on the worn surface are less than that of 5 L/min. When the nitrogen flux increases to 15 L/min, the coating worn surface is smooth with shallow furrows (Fig. 11(c)), indicating that the coating has good anti-wear property. Plenty of TiN and Ti_2N hard phases synthesized in the coating significantly improve the microhardness of the coating, and also enhance the ability of resisting micro-cutting and ploughing in the sliding friction process. When nitrogen flux is too large (20 L/min), many debris and peeling offs can be seen on the surface of the coating (Fig. 11(d)). This can be attributed to the excessive nitrogen flux which might result in turbulence phenomenon on substrate surface. The air involved in the molten pool does not have sufficient time to escape, thus the micro-cracks and holes generated. Under the action of the reciprocating grinding force, the micro-cracks propagate and eventually lead to the bulk peeling off of the coating.

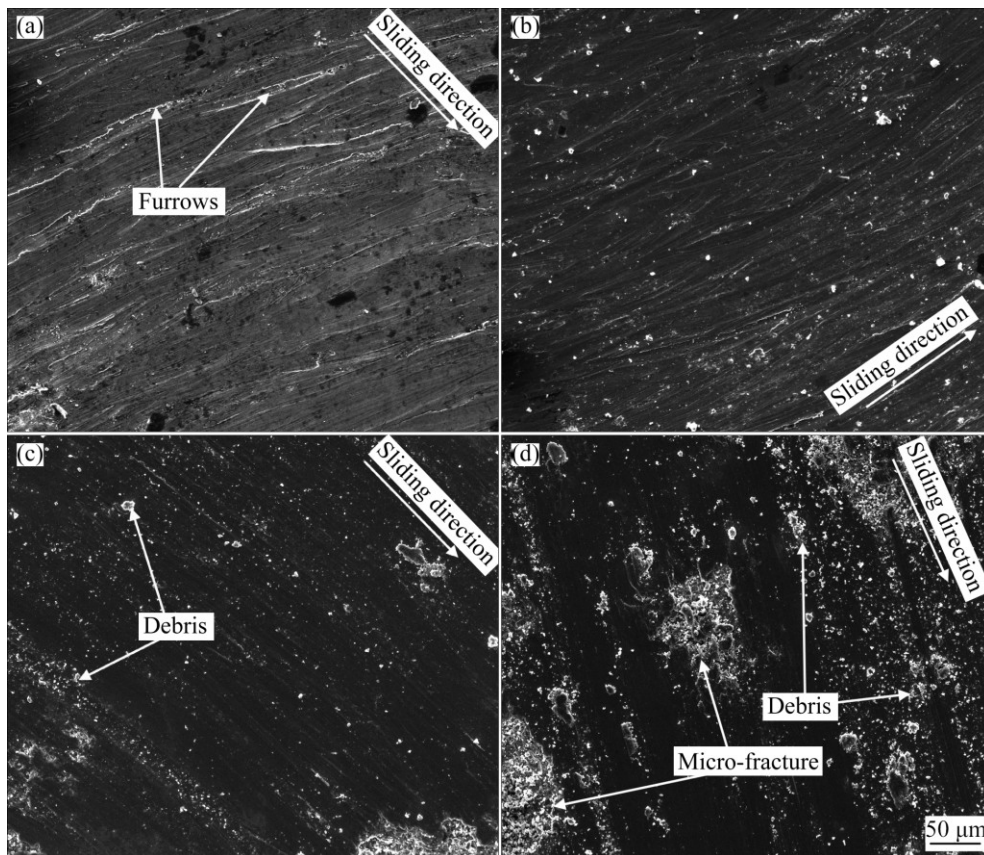


Fig. 11 Worn morphologies of coating under different nitrogen fluxes: (a) 5 L/min; (b) 10 L/min; (c) 15 L/min; (d) 20 L/min

4 Conclusions

1) The output voltage x and nitrogen flux l present significant effects on majority of the evaluation indexes such as TOC, friction coefficient (COF) and wear mass loss (I_d), while the specific strengthening time s has significant effect on POC and has minor effect on the other indexes.

2) The optimal process parameter was obtained as follows: output voltage (x , 60 V), nitrogen flux (l , 15 L/min) and specific strengthening time (s , 3 min/cm²).

3) The variation of wear mass loss (I_d) by the variation of the output voltage x and nitrogen flux l is attributed to the changing of wear mechanisms of TiN coatings. The main wear mechanism of TiN coating prepared by ESD is micro-cutting wear accompanied by micro-fracture wear.

References

- [1] STOJADINOVIC S, VASILIC R, PETKOVIC M, KASALICA B, BELCA I, ZEKIC A, ZEKOVIC L. Characterization of the plasma electrolytic oxidation of titanium in sodium metasilicate [J]. Applied Surface Science, 2013, 265: 226–233.
- [2] TACIKOWSKI M, MORGIEL J, BANASZEK M, CYMERMAN K, WIERZCHON T. Structure and properties of diffusive titanium nitride layers produced by hybrid method on AZ91D magnesium alloy [J]. Transactions of Nonferrous Metals Society of China, 2014, 24: 2767–2775.
- [3] HONG Li, ZHANG Chao, LIU Hong-bin, LI Miao-quan. Bonding interface characteristic and shear strength of diffusion bonded Ti-17 titanium alloy [J]. Transactions of Nonferrous Metals Society of China, 2015, 25: 80–87.
- [4] DURDU S, AKTUG S L, KORKMAZ K. Characterization and mechanical properties of the duplex coatings produced on steel by electro-spark deposition and micro-arc oxidation [J]. Surface and Coating Technology, 2013, 236: 303–308.
- [5] LECLAIR P, BERERA G P, MOODERA J S. Titanium nitride thin films obtained by a modified physical vapor deposition process [J]. Thin Solid Films, 2000, 376(1): 9–15.
- [6] LIN Xiao-xuan, ZHAO Gao-ling, WU Li-qing, DUAN Gang-feng, HAN Gao-rong. TiN thin films for energy-saving application prepared by atmospheric pressure chemical vapor deposition [J]. Journal of Alloys and Compounds, 2010, 502(1): 195–198.
- [7] KRISCHOK S, BLANK C, ENGEL M, GUTT R, ECKE G, SCHAWOHL J, LIEFEITH K. Influence of ion implantation on titanium surfaces for medical applications [J]. Surface Science, 2007, 601(18): 3856–3860.
- [8] ASHRAFIZADEH A, ASHRAFIZADEH F. Structural features and corrosion analysis of thermally oxidized titanium [J]. Journal of Alloys and Compounds, 2009, 480(2): 849–852.
- [9] XI Ying-xue, FAN Hui-qing, LIU Wei-guo. The effect of annealing treatment on microstructure and properties of TiN films prepared by unbalanced magnetron sputtering [J]. Journal of Alloys and Compounds, 2010, 496(1): 695–698.
- [10] LU Y M, HWANG W S, LIU W Y, YANG J S. Effect of RF power on optical and electrical properties of ZnO thin film by magnetron

- sputtering [J]. Materials Chemistry and Physics, 2001, 72(2): 269–272.
- [11] FRANGINI S, MASCI A, DI BARTOLOMEO A. Cr₇C₃-based cermet coating deposited on stainless steel by electrospark process: Structural characteristics and corrosion behavior [J]. Surface and Coatings Technology, 2002, 149(2): 279–286.
- [12] FRANGINI S, MASCI A. FeAl based coatings deposited by the electrospark technique: Corrosion behavior in molten (Li+K) carbonate [J]. Surface and Coatings Technology, 2004, 184(1): 31–39.
- [13] AGARWAL A, DAHOTRE N B. Pulse electrode deposition of superhard boride coatings on ferrous alloy [J]. Surface and Coatings Technology, 1998, 106(2): 242–250.
- [14] WANG R J, QIAN Y Y, LIU J. Structural and interfacial analysis of WC92–Co8 coating deposited on titanium alloy by electrospark deposition [J]. Applied Surface Science, 2004, 228(1): 405–409.
- [15] TANG C B, LIU D X, WANG Z, GAO Y. Electro-spark alloying using graphite electrode on titanium alloy surface for biomedical applications [J]. Applied Surface Science, 2011, 257(15): 6364–6371.
- [16] HAO Jian-jun, PENG Hai-bin, HUANG Ji-hua, MA Yue-jin, LI Jian-chang. TiN/Ti composite coating deposited on titanium alloy substrate by reactive electric-spark [J]. Transactions of The China Welding Institution, 2009, 30(11): 69–72. (in Chinese)
- [17] HONG Xiang, TAN Ye-fa, WANG Xiao-long, TAN Hua, XU Ting. Effects of nitrogen flux on microstructure and tribological properties of in-situ TiN coatings deposited on TC11 titanium alloy by electrospark deposition [J]. Transactions of Nonferrous Metals Society of China, 2015, 25: 3329–3338.
- [18] GUO S, JIN Y, ZHAO H. Determination of phase composition and mass fraction of bulk zinc–aluminum based magnesium–lead alloy [J]. Materials Review, 2009, 23(4): 64–67.
- [19] JIA Sheng-kai, ZOU Yong, XU Ji-yuan, WANG Jing, YU Lei. Effect of TiO₂ content on properties of Al₂O₃ thermal barrier coatings by plasma spraying [J]. Transactions of Nonferrous Metals Society of China, 2015, 25: 175–183.
- [20] SHAN Lei, ZHANG Yang-rong, WANG Yong-xin, LI Jin-long, JIANG Xin, CHEN Jian-min. Corrosion and wear behaviors of PVD CrN and CrSiN coatings in seawater [J]. Transactions of Nonferrous Metals Society of China, 2016, 26: 175–184.

工艺参数对 TC11 钛合金表面电火花沉积 TiN 涂层显微组织和磨损性能的影响

洪翔, 冯柯, 谭业发, 王小龙, 谭华

解放军理工大学 野战工程学院, 南京 210007

摘要: 系统研究了工艺参数(放电电压 x , 氮气流量 l 和比强化时间 s)对电火花沉积 TiN 涂层显微组织和耐磨性能的影响规律。以涂层厚度(TOC)、TiN 含量(CON)和孔隙率(POC)来表征涂层显微组织。建立了一个数学模型来确定对涂层显微组织和耐磨性能影响最显著的参数。结果表明: 放电电压 x 和氮气流量 l 对大多数指标都有较大影响, 比如涂层厚度、摩擦因数(COF)和磨损失重(I_d), 而比强化时间 s 对孔隙率影响较大, 对其他指标影响不显著。试验得到最佳工艺参数为: 放电电压 60 V, 氮气流量 15 L/min 和比强化时间 3 min/cm²。由于涂层磨损机制的变化, 涂层磨损失重随放电电压和氮气流量的变化而变化。在最佳工艺参数下, TiN 涂层的主要磨损机理为微观切削磨损伴随轻微断裂磨损。

关键词: 电火花沉积; 氮化钛; 涂层; 耐磨性能; 统计模型; 工艺参数

(Edited by Yun-bin HE)